Acta Pharmaceutica Sinica B 2018;8(4):687–697

Chinese Pharmaceutical Association
Institute of Materia Medica, Chinese Academy of Medical Sciences

Acta Pharmaceutica Sinica B

www.elsevier.com/locate/apsb
www.sciencedirect.com

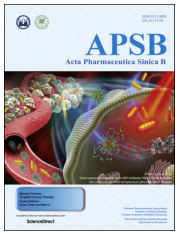

ORIGINAL ARTICLE

Epigenetic modification in histone deacetylase deletion strain of *Calcarisporium arbuscula* leads to diverse diterpenoids

Jian Bai[a], Rong Mu[a], Man Dou[a], Daojiang Yan[a], Bingyu Liu[a], Qian Wei[a], Jun Wan[a], Yi Tang[a,b], Youcai Hu[a,*]

[a]*State Key Laboratory of Bioactive Substance and Function of Natural Medicines, Institute of Materia Medica, Chinese Academy of Medical Sciences & Peking Union Medical College, Beijing 100050, China*
[b]*Department of Chemical and Biomolecular Engineering, Department of Chemistry and Biochemistry, University of California, Los Angeles, CA 90095, USA*

Received 27 August 2017; received in revised form 21 September 2017; accepted 15 October 2017

KEY WORDS

Calcarisporium arbuscula;
Calcarisporic acids;
Pimarane;
Diterpenoid;
Matrix metalloproteinases inhibitor;
Epigenetic genome mining

Abstract Epigenetic modifications have been proved to be a powerful way to activate silent gene clusters and lead to diverse secondary metabolites in fungi. Previously, inactivation of a histone H3 deacetylase in *Calcarisporium arbuscula* had led to pleiotropic activation and overexpression of more than 75% of the biosynthetic genes and isolation of ten compounds. Further investigation of the crude extract of *C. arbuscula ΔhdaA* strain resulted in the isolation of twelve new diterpenoids including three cassanes (**1–3**), one cleistanthane (**4**), six pimaranes (**5–10**), and two isopimaranes (**11** and **12**) along with two know cleistanthane analogues. Their structures were elucidated by extensive NMR spectroscopic data analysis. Compounds **2** and **4** showed potent inhibitory effects on the expression of MMP1 and MMP2 (matrix metalloproteinases family) in human breast cancer (MCF-7) cells.

*Corresponding author.
E-mail address: huyoucai@imm.ac.cn (Youcai Hu).

Peer review under responsibility of Institute of Materia Medica, Chinese Academy of Medical Sciences and Chinese Pharmaceutical Association.

https://doi.org/10.1016/j.apsb.2017.12.012

1. Introduction

Calcarisporium arbuscula, an endophytic fungus lives in the flesh of healthy fruit-bodies of mushrooms[1], mainly produces the adenosine triphosphate synthase inhibitors aurovertins B and D, which structurally contain a 2,6-dioxabicyclo[3.2.1]-octane ring[2–4]. In our prior genome mining investigation[5], genome sequencing of *C. arbuscula* revealed a large number of potential secondary metabolite gene clusters (68, of which 9 contain terpene synthases), which are significantly more than the two predominant metabolites aurovertins B and D, suggesting that most gene clusters are silent or lowly expressed in axenic cultures. Epigenetic modifications have been proved to be a powerful way to activate silent gene clusters in fungi[6–10]. Deletion of *hdaA*, which encodes a histone deacetylase (HDAC), has led to the globally pleiotropic activation and overexpression of more than 75% of the biosynthetic genes and the isolation of diverse ten compounds of which four possess new structures, including three tricyclic diterpenes and a novel meroterpenoid derived from the esterification between an anthraquinone and a cassane diterpene[5]. So far, diterpenoids have exhibited diverse structural features and a wide range of interesting biological activities[11,12], such as cytotoxic[13,14], antimicrobial[15,16], anti-inflammatory[17], and antiviral[18–20] properties, attracting more and more attention.

Careful analysis of the crude extract from the *C. arbuscula* Δ*hdaA* strain by UPLC–MS showed the presence of numerous minor ingredients that could not be identified due to sample limitations. To further explore the potential of the mutant strain Δ*hdaA* and ongoing search for diverse new bioactive natural products, we fermented in a larger scale using potato dextrose agar (PDA) culture. Subsequently, investigation of the PDA fermentation extract resulted in the isolation of twelve new diterpenoids including three cassanes (**1**–**3**), one cleistanthane (**4**), six pimaranes (**5**–**10**), and two isopimaranes (**11** and **12**), together with two known cleistanthanes analogues (**13** and **14**, Fig. 1). Herein, details of the isolation, structure characterization, and bioactivities of **1**–**14** are reported.

2. Results and discussion

Compound **1** was isolated as a colorless amorphous solid with $[\alpha]_D^{20}$ +30.0 (*c* 0.10, MeOH). The IR spectrum of **1** showed absorption bands for hydroxyl (3490 cm^{-1}), carbonyl (1724 cm^{-1}), and carbon-carbon double bonds moieties (1649 cm^{-1}). Its molecular formula was determined as $C_{20}H_{28}O_5$ by negative HR-ESI-MS at *m/z* 347.1864 $[M–H]^-$ (Calcd. for $C_{20}H_{27}O_5$, 347.1864) combined with NMR spectroscopic data (Tables 1 and 2). The ^1H NMR spectrum of **1** showed signals attributable to a vinyl group [δ_H 6.25 (dd, J = 17.7 and 10.9 Hz, H-16), 5.09 (d, J = 17.7 Hz, H-17a), and 4.92 (d, J = 10.9 Hz, H-17b)], an olefinic proton [δ_H 5.66 (br s, H-12)], an oxygen-bearing methine [δ_H 4.34 (m, H-3)], a secondary methyl [δ_H 1.08 (d, J = 7.0 Hz, H-15)] and two tertiary methyl [δ_H 1.50 (s, H-18) and 0.89 (s, H-20)]. The ^{13}C NMR and HSQC data revealed the presence of 20 carbons, including three methyls, four methylenes, four methines (including one *O*-methine), three sp^3 quaternary carbons with one oxygenated, four olefinic carbons accounting for an olefin and a vinyl group, a carboxylic carbon (δ_C 175.1), and a ketone carbon (δ_C 211.7). These data accounted for all the NMR resonances of **1** and four of the seven unsaturation degrees, indicating **1** as a tricyclic compound.

Analysis of the ^1H–^1H COSY NMR data (Fig. 2) of **1** identified the C-1–C-3 moiety, the C-16–C-17 vinyl group, and the C-7/8/9/11/12 unit with the C-14–C-15 fragment attached to C-8. In the HMBC spectrum (Fig. 2) of **1**, correlations from the olefinic proton H-16 to C-12, C-13, and C-14 indicated that C-13 was connected to C-12, C-14, and C-16, respectively, establishing a cyclohexene ring with a vinyl and a methyl groups located at C-13 and C-14, respectively. HMBC correlations from the methyl H_3-20 to C-1, C-5, C-9, and C-10 led to the connections of C-1, C-5, C-9, and C-20 to C-10. The HMBC correlations of H_3-18/C-3, C-4, C-5, and C-19 and H_2-7/C-5 and C-6 located two hydroxy groups at C-3 and C-5, respectively, a carboxyl group at C-19, and a ketone group at C-6, establishing the tricyclic cassane type diterpene skeleton. Based on these data, the planar structure of **1** was established as shown in Fig. 1 which is closely resemble to sonomolide B[15] and hawaiinolide F[14].

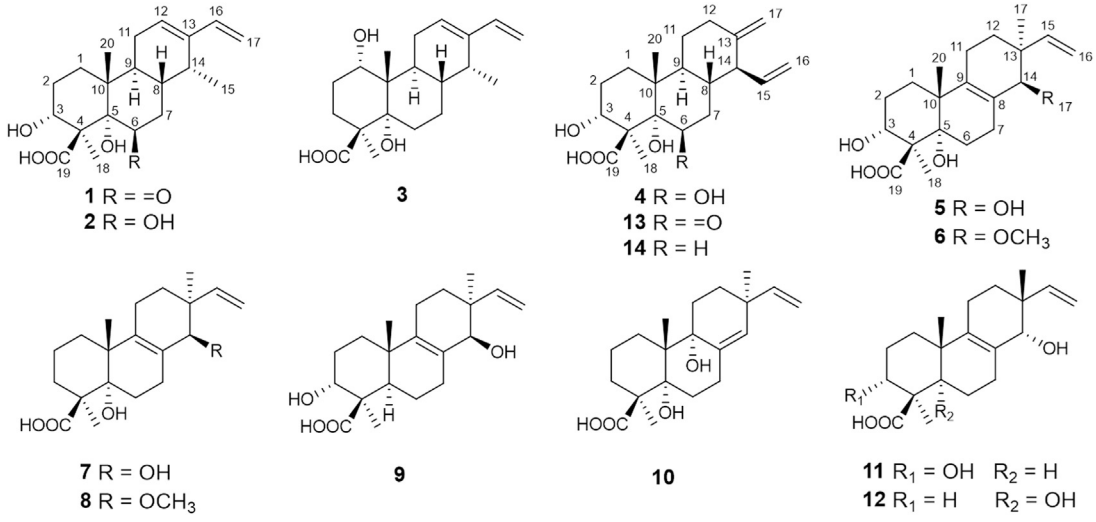

Figure 1 Structures of compounds **1**–**14**.

Table 1 ^{13}C NMR spectroscopic data (δ) for compounds **1**–**12**[a] (δ in ppm).

No.	1	2	3	4	5	6	7	8	9	10	11	12
1	28.2	29.21	71.1	28.6	25.9	25.6	31.1	30.8	31.6	28.4	31.3	30.0
2	24.3	26.3	26.45	26.0	27.7	27.8	20.1	20.1	27.7	19.7	27.7	20.0
3	79.4	73.2	26.43	72.9	73.7	73.8	32.8	32.9	71.3	33.5	71.4	32.9
4	59.3	49.1	48.6	51.0	51.1	51.2	49.7	49.8	48.7	50.4	49.0	49.9
5	82.2	78.9	77.7	78.0	80.5	80.1	77.1	76.9	46.5	81.2	46.7	76.9
6	211.7	69.8	27.8	69.2	26.4	26.4	26.3	26.3	21.3	30.0	21.7	26.8
7	42.0	32.7	24.2	35.0	26.8	26.7	27.2	27.1	31.4	27.8	32.0	26.7
8	39.1	29.17	33.5	35.4	128.8	128.1	129.0	128.2	129.8	137.5	128.7	128.0
9	35.8	35.8	29.3	45.8	138.8	138.5	139.2	139.2	140.5	78.5	140.3	137.9
10	45.2	41.6	42.8	41.1	44.6	44.6	44.4	44.6	39.4	43.4	39.2	44.4
11	26.9	24.9	24.4	26.6	22.1	22.2	22.1	22.1	21.7	27.6	22.0	22.6
12	128.8	129.3	128.7	35.7	30.1	31.6	30.2	31.5	32.3	32.9	27.6	28.4
13	142.6	141.5	141.1	151.0	40.6	41.1	40.6	41.1	40.7	40.0	40.4	40.4
14	33.2	31.6	31.6	53.6	77.2	88.5	77.2	88.6	77.9	132.8	76.0	76.3
15	14.8	15.0	14.6	139.8	145.8	146.4	145.8	146.3	147.7	146.6	147.9	147.5
16	139.6	139.0	138.7	116.7	112.3	112.3	112.3	112.4	111.8	113.7	111.8	112.0
17	110.5	110.1	109.6	106.2	23.0	21.8	22.9	21.9	19.6	29.7	21.1	21.5
18	19.4	20.6	24.0	19.9	20.4	20.5	24.5	24.5	24.6	24.2	24.6	24.6
19	175.1	178.4	179.0	177.5	178.7	178.9	181.0	181.1	181.3	180.2	181.4	181.2
20	15.5	15.1	14.5	15.0	22.9	22.9	22.6	22.6	17.9	19.2	17.9	22.5
OMe						62.0		62.1				

[a]NMR data (δ) were measured at 125 MHz in CD_3OD for **1**, **5**, **6**, **8**–**12**; at 150 MHz in CD_3OD for **7**; and at 150 MHz in DMSO-d_6 for **2**–**4**.

The relative configuration of **1** was deduced by analysis of NOESY spectrum. NOESY correlations (Fig. 3) of H_3-20 with H-8 and H-2β (δ_H 2.03) and of H-3 with H-2β indicated that these protons were in the β-orientation, whereas those of H_3-15 with H-9 suggested the α-axial orientation of the methyl at C-14. NOESY cross peaks of OH-5 with H-9 and H_3-18, indicating the α-orientation for OH-5 and Me-18. Thus, the relative configuration of **1**, which was very similar as those of hawaiinolides F and G[14], was established.

The absolute configuration of **1** was determined by analysis of its CD spectrum. The negative Cotton effect observed at 320 nm in the CD spectrum (Fig. 4) is associated with the $n\rightarrow\pi^*$ transition of the cyclohexanone chromophore[13,21,22]. On the basis of the octant rule for cyclohexanones, the 5 *S* absolute configuration was determined. Combining the established relative configuration, the absolute configuration of **1** was deduced to be 3 *R*, 4 *S*, 5 *S*, 8 *S*, 9 *S*, 10 *R*, 14 *R*. Therefore, **1** was determined as 3*R*, 5*S*-dihydroxy-6-oxo-14*R*-cassane-12, 16-dien-19-oic acid and named calcarisporic acid A.

Compound **2** possesses the molecular formula $C_{20}H_{30}O_5$ as determined by negative HR-ESI-MS at *m/z* 349.2030 $[M–H]^-$ (Calcd. for $C_{20}H_{29}O_5$, 349.2020) and NMR spectroscopic data. Comparing the 1D NMR spectra (Tables 1 and 2) of **2** with those of **1**, signals due to an oxygenated methine were observed at δ_H 4.04 (br s, H-6) and δ_C 69.8 in the NMR spectra of **2**, with the disappearance of the ketone carbon at δ_C 211.7 (C-6) in **1**. The HMBC correlations from the oxygenated methine proton at δ_H 4.04 (br s, H-6) to C-4, C-5, C-7, C-8, and C-10, indicated the location of the hydroxyl group at C-6. According to NOESY correlations, the relative configuration of **2** was same as that of **1**, except for the presence of correlation of H-6 with H_3-18, which suggested the β-configuration of OH-6. Therefore, **2** was established as 3α, 5α, 6β-trihydroxy-15α-cassane-12, 16-dien-19-oic acid and named calcarisporic acid B.

The molecular formula of compound **3** was determine as $C_{20}H_{30}O_4$ on the basis of negative HR-ESI-MS at *m/z* 333.2083 $[M–H]^-$ (Calcd. for $C_{20}H_{29}O_4$, 333.2071). The ^{1}H NMR and ^{13}C NMR spectroscopic data (Tables 1 and 2) of **3** were similar to those of **2**. The major difference was that signals for a methylene at δ_C 27.8 (C-6), δ_H 2.03 (td, J = 13.8, 2.4 Hz, H-6a), and δ_H 1.62 (m, H-6b) in **3** replaced resonances for an oxygenated methine at δ_C 69.8 (C-6) and δ_H 4.04 (br s, H-6) in **2**, which were verified by HMBC correlations from H_2-6 to C-5, C-7, C-8, and C-10. HMBC correlations from H-1 (δ_H 3.57) to C-3, C-5, C-10, and C-20, suggested that C-1 was substituted by a hydroxy group. In addition, the relative configuration of **3** was deduced from NOESY correlations and by comparison to that of **2**. NOESY correlations of H_3-20 with H-1 and H-8 indicated the β-configuration of H-1, whereas those of OH-5 with H_3-18, OH-1, and H-9, and of H_3-15 with H-9 revealed that they were in the α-orientation. Thus, **3** was elucidated as 1α, 5α-dihydroxy-15α-cassane-12, 16-dien-19-oic acid and designated as calcarisporic acid C.

Compound **4**, colorless needles with $[\alpha]_D^{20}$ +10.2 (*c* 0.17, MeOH), was determined to have the molecular formula of $C_{20}H_{30}O_5$ by negative HR-ESI-MS at *m/z* 349.2031 $[M–H]^-$ (Calcd. for $C_{20}H_{29}O_5$, 349.2020). The ^{1}H NMR and ^{13}C NMR spectroscopic data (Tables 1 and 2) showed the presence of two tertiary methyl, five methylenes, five methines (including two *O*-methines), three sp^3 quaternary carbons with one oxygenated, four olefinic carbons accounting for an exocyclic olefin [δ_H 4.64 (d, J = 1.1 Hz, H-17a), and 4.48 (br s, H-17b); δ_C 106.2 (C-17) and 151.0 (C-13)] and a vinyl group [δ_H 5.62 (ddd, J = 17.2, 9.8 and 9.8 Hz, H-15), 5.13 (dd, J = 10.2 and 2.0 Hz, H-16a), and 4.98 (dd, J = 17.2 and 2.0 Hz, H-16b); δ_C 139.8 (C-15) and 116.7 (C-16)], and one carboxylic carbon [δ_C 177.5 (C-19)]. Comparison of the NMR spectroscopic data of **4** with those of **2** suggested that **4** possessed the same A and B ring units as those in **2**. Analysis of the ^{1}H–^{1}H COSY NMR data (Fig. 2) of **4** revealed the C-6/7/8/9/11/12 unit with the C-14–C-16 fragment attached to C-8. HMBC correlations (Fig. 2) of H_2-17/C-12, C-13, and C-14, and H-15/C-13, C-14, and C-8 confirmed that the olefinic methylene and vinyl

Table 2 ^{1}H NMR spectroscopic data (δ) for compounds **1**–**4**[a] (δ in ppm, J in Hz).

No.	1	2	3	4
1	1.94, overlap 1.59, m	1.70, td (13.8, 3.5) 1.14, d (12.5)	3.57, d (3.0)	1.66, overlap 1.26, br d (12.8)
2	2.31, m 2.03, overlap	1.98, overlap 1.56, d (11.6)	2.10, overlap 1.64, overlap	1.98, overlap 1.57, m
3	4.34, br d (5.5)	4.22, br s	1.72, td (13.7, 4.0) 1.50, overlap	5.21, br s
6		4.04, br s	2.03, td (13.8, 2.4) 1.62, overlap	3.92, br s
7	3.14, t (12.9) 2.09, dd (13.0, 4.9)	2.11, m 1.35, overlap	1.87, overlap 1.24, br d (12.1)	1.62, overlap
8	1.94, overlap	1.77, m	1.52, overlap	1.41, m
9	2.71, m	2.09, m	2.56, m	1.72, overlap
11	2.22, m 2.02, overlap	2.01, overlap 1.95, overlap	2.12, overlap 1.84, overlap	1.70, overlap 1.00, qd (13.0, 3.6)
12	5.66, br s	5.63, t (3.5)	5.63, t (3.8)	2.35, d (12.9) 1.98, overlap
14	2.47, m	2.32, m	2.38, m	2.25, t (9.8)
15	1.08, d (7.0)	0.87, d (6.8)	0.92, d (6.9)	5.62, ddd (17.2, 9.8, 9.8)
16	6.25, dd (17.7, 10.9)	6.20, dd (17.6, 10.9)	6.20, dd (17.6, 10.9)	5.13, dd (10.2, 2.0) 4.98, dd (17.2, 2.0)
17	5.09,d (17.7) 4.92, d (10.9)	5.08,d (17.6) 4.90, d (10.9)	5.07,d (17.6) 4.89, d (10.9)	4.64, d (1.1) 4.48, br s
18	1.50, s	1.36, s	1.12, s	1.32, s
20	0.89, s	0.96, s	0.70, s	0.91, s
1-OH			5.50, d (4.0)	
3-OH		6.23, br s		6.23, d (2.5)
5-OH		6.10, br s	5.15, s	6.20, br s
6-OH				7.21, br s
19-OH			12.11, s	14.32, br s

[a]NMR data (δ) were measured at 500 MHz in CD_3OD for **1** and at 600 MHz in DMSO-d_6 for **2**–**4**.

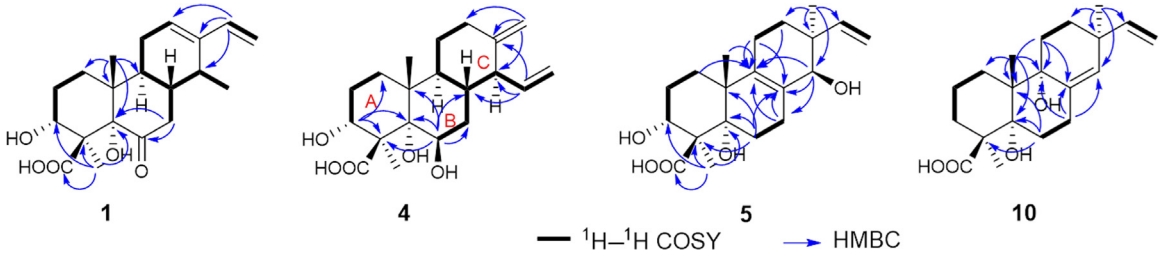

Figure 2 ^{1}H–^{1}H COSY and key HMBC correlations of compounds **1**, **4**, **5** and **10**.

group connected to C-13 and C-14, respectively, establishing a cyclohexane of C ring moiety with an exocyclic olefin at C-13/C-17 and a vinyl group attached to C-13 fused to the B ring unit at C-8/C9. Thus, the planar structure of **4** was established (Fig. 1), a tricyclic cleistanthane diterpene, which closely resembled that of zythiostromic acid A isolated from *Zythiostroma* sp. with $[\alpha]_D^{20}$ −31.7 (*c* 0.35, MeOH)[23]. This suggested that the two compounds are diastereomers. Comparison of the chemical shifts and coupling constants in the ^{1}H NMR spectra of **4** and zythiostromic acid A indicated difference only in the signals attribute to H-14 and H-15. This suggested that **4** was the C-14 epimer of zythiostromic acid A, which were confirmed by NOESY correlations (Fig. 3) of H-14 with H-9, and of H-8 with H-15 and H_3-20, while other NOESY correlations of **4** were the same as those of zythiostromic acid A. Therefore, **4** was established as 3α, 5α, 6β-trihydroxy-15β-cleistanthane-13(17), 15-dien-19-oic acid and named calcarisporic acid D.

Compound **5** was obtained as colorless needles. Its molecular formula was $C_{20}H_{30}O_5$, as determined by negative HR-ESI-MS at *m/z* 349.2036 $[M–H]^-$ (Calcd. for $C_{20}H_{29}O_5$, 349.2020). Analysis of its ^{1}H and ^{13}C NMR data (Tables 1 and 3) revealed the presence of three tertiary methyls, six methylenes, two oxygenated methines, four sp^3 quaternary carbons with one oxygenated, four olefinic carbons accounting for a tetra-substituted olefin and a vinyl group, and a carboxylic carbon (δ_C 178.7). Comparison of the NMR spectroscopic data of **5** with those of **2** suggested that **5** possessed the same A ring moiety as **2**. Interpretation of the ^{1}H–^{1}H COSY NMR data (Fig. 2) of **5** identified the C-6–C-7 moiety, the C-11–C-12 unit, and the C-15–C-16 vinyl group. HMBC correlations (Fig. 2) from H-6 to C-4, C-5, and C-10 suggested that the

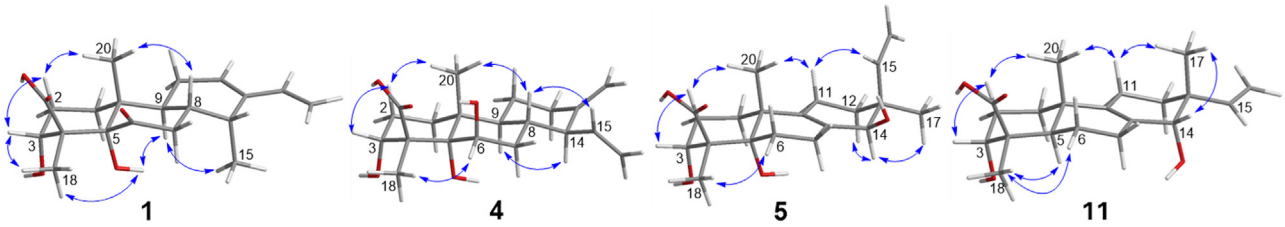

Figure 3 Key NOESY correlations of compounds **1**, **4**, **5** and **11**.

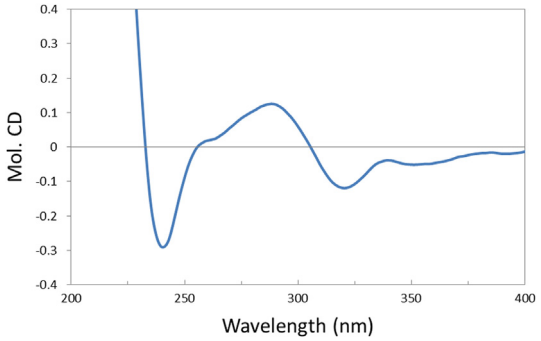

Figure 4 CD spectrum of **1** in MeOH.

C-6–C-7 moiety was attached to C-5. HMBC correlations from H-1, H_3-20, and H-7 to C-9, and from H-6 and H-7 to C-8 suggested that the tetra-substituted olefin C-8 and C-9 were connected to C-7 and C-9, respectively, establishing a cyclohexene of B ring moiety fused to the A ring unit at C-5/C10. HMBC correlations from H-14 to C-7, C-8, and C-9, and from H-11 to C-8, C-9, and C-10 indicated that the oxygenated C-14 and C-11 were attached to C-8 and C-9, respectively. HMBC cross peaks from H_3-17 to C-12, C-13, C-14, and C-15 led to the connections of C-12, C-14, C-15, and C-17 to C-13, establishing the C-8/C-9 fused cyclohexene of C ring unit with a methyl and a vinyl group both attached to C-13. Thus, the planar structure of **5** was established as shown in Fig. 1, a tricyclic pimarane diterpene. The relative configuration of **5** was confirmed by NOESY spectrum. NOESY correlations (Fig. 3) of H-11β (δ_H 1.96) with H_3-20 and H-15, and of H-2β (δ_H 2.31) with H-3 and H_3-20 suggested that these protons were in the β-configuration, whereas those of H-14 with H_3-17 and H-12α (δ_H 1.44) indicated the α-axial configuration of H-14. NOESY correlation of Me-18 with H-3 and H-6α (δ_H 1.92) and the absence of NOESY correlation between Me-18 and the axial Me-20 revealed that the carboxylic group at C-4 was in the β-axial orientation. Thus, **5** was elucidated as 3α, 5α, 14β-trihydroxy-pimarane-8(9), 15-dien-19-oic acid and designated as calcarisporic acid E.

The molecular formula of compound **6** was established as $C_{21}H_{32}O_5$ by negative HR-ESI-MS at *m/z* 363.2182 $[M–H]^-$ (Calcd. for $C_{21}H_{31}O_5$, 363.2177). The ^1H and ^{13}C NMR spectra (Tables 1 and 3) of **6** showed close resemblance to those of **5**, except for the presence of an additional methoxy group [δ_H 3.51 (3 H, s), δ_C 62.0] relative to **5**. It was observed that the resonance for C-14 was downfield-shifted from δ_C 77.2 in **5** to δ_C 88.5 in **6**, and the protons of methoxy group showed HMBC correlation with C-14, which suggested that **6** was the 14-methoxy derivative of **5**. The relative configuration of **6** was the same as that of **5** according to NOESY correlations. Therefore, **6** was elucidated as 3α,5α-dihydroxy-14β-methoxy-pimarane-8(9), 15-dien-19-oic acid and designated as calcarisporic acid F.

Compound **7** was assigned the molecular formula $C_{20}H_{30}O_4$ by negative HR-ESI-MS at *m/z* 333.2077 $[M–H]^-$ (Calcd. for $C_{20}H_{29}O_4$, 333.2071), one less oxygen than that of **5**. Comparison of the NMR data of **7** with those of **5** indicated that an *O*-methine [δ_H 4.10, δ_C 73.7] at C-3 in **5** was replayed by a methylene [δ_H 1.83 and 1.74, δ_C 32.8] in **7**. This suggested that **7** was the 3-dehydroxy analog of **5**, which was confirmed by HMBC correlations from H_2-3 to C-1, C-2, C-4, and C-5. NOESY correlations of H-11β (δ_H 1.94) with H_3-20 and H-15, of H-14 with H_3-17 and H-12α (δ_H 1.43), and of H_3-18 with H-3α (δ_H 1.83), H-3β (δ_H 1.74), and H-6α (δ_H 1.93) indicated that the relative configuration of **7** was similar as that of **5**. Thus, **7** was established as 5α,14β-dihydroxy-pimarane-8(9), 15-dien-19-oic acid and named calcarisporic acid G.

Compound **8** was determined to have the molecular formula of $C_{21}H_{32}O_4$ by negative HR-ESI-MS at *m/z* 347.2239 $[M–H]^-$ (Calcd. for $C_{21}H_{31}O_4$, 347.2228). The NMR data (Tables 1 and 3) of **8** were closely similar to those of **7**. The major differences were that an additional methoxy group was presented in **8**, and the resonance for C-14 was downfield-shifted by 11.4 ppm in comparison with **7**. This indicated that **8** was the 14-methoxy derivative of **7**, which was verified by HMBC correlations from H-14 to the additional methoxy group (δ_C 62.1), C-8, C-9, C-13, and C-15. The relative configuration of **8** was identical with that of **7** according to NOESY spectrum. Consequently, **8** was elucidated as 5α-hydroxy-14β-methoxy-pimarane-8(9), 15-dien-19-oic acid and designated as calcarisporic acid H.

The molecular formula of compound **9** was deduced to be $C_{20}H_{30}O_4$ by negative HR-ESI-MS at *m/z* 333.2077 $[M–H]^-$ (Calcd. for $C_{20}H_{29}O_4$, 333.2071). The ^1H and ^{13}C NMR spectra (Tables 1 and 4) of **9** showed close resemblance to those of **5**, with the exception of the signals assigned to C-5, where the oxygenated quaternary carbon (δ_C 80.5) in **5** was replayed by a methine [δ_H 1.79 (d, J = 12.2 Hz), and δ_C 46.5] in **9**. This suggested that **9** was the 5-dehydroxy analog of **5**, which was confirmed by HMBC correlations from H-5 (δ_H 1.79) to C-1, C-4, C-6, C-10, C-18, C-19, and C-20. NOESY correlations of H_3-18 with H-5 (δ_H 1.79) and H-3, of H-11β (δ_H 1.92) with H_3-20 and H-15, and of H-14 with H_3-17 and H-12α (δ_H 1.43) indicated that the relative configuration of **9** was in accordance with that of **5**. Therefore, **9** was elucidated as 3α,14β-dihydroxy-pimarane-8(9), 15-dien-19-oic acid and designated as calcarisporic acid I.

Compound **10** was assigned the molecular formula $C_{20}H_{30}O_4$ by negative HR-ESI-MS at *m/z* 333.2069 $[M–H]^-$ (Calcd. for $C_{20}H_{29}O_4$, 333.2071). The ^1H and ^{13}C NMR data (Tables 1 and 4) showed the presence of three tertiary methyls, seven methylenes, five sp^3 quaternary carbons with two oxygenated, four olefinic carbons accounting for a trisubstituted olefin and a vinyl group, and a carboxylic carbon (δ_C 180.2). Comparison of the NMR spectroscopic data of **10** with those of **7** suggested that **10** possessed the same A ring unit as **7**. Analysis of the ^1H–^1H COSY spectrum (Fig. 2) of **10** revealed the C-6–C-7 moiety, the C-11–C-12 unit, and the C-16–C-17 vinyl group. HMBC

Table 3 ^{1}H NMR spectroscopic data (δ) for compounds **5–8**[a] (δ in ppm, J in Hz).

No.	5	6	7	8
1	1.97, overlap	1.96, overlap	1.78, dd (12.9, 4.1)	1.77, overlap
	1.41, br d (12.5)	1.38, overlap	1.42, overlap	1.41, overlap
2	2.31, m	2.30, m	1.97, overlap	1.96, overlap
	1.73, dd (14.4, 3.0)	1.71, m	1.46, overlap	1.45, overlap
3	4.10, br s	4.07, br s	1.83, d (12.7)	1.83, d (12.8)
			1.74, overlap	1.72, overlap
6	2.48, m	2.47, m	2.49, m	2.50, m
	1.92, overlap	1.94, overlap	1.93, overlap	1.94, overlap
7	2.55, m	2.51, m	2.57, m	2.51, m
	1.93, overlap	1.93, overlap	1.95, overlap	1.96, overlap
11	2.02, overlap	1.99, overlap	1.94, overlap	1.92, overlap
	1.96, overlap	1.94, overlap		
12	1.67, m	1.59, m	1.66, m	1.58, m
	1.44, overlap	1.47, overlap	1.43, overlap	1.46, overlap
14	3.47, br s	3.24, br s	3.48, br s	3.24, br s
15	5.76, dd (17.7, 11.0)	5.80, dd (17.7, 11.0)	5.77, dd (17.7, 11.0)	5.80, dd (17.7, 11.0)
16	4.96, br d (17.7)	4.99, dd (17.7, 1.4)	4.96, dd (17.7, 1.4)	4.99, dd (17.7, 1.0)
	4.93, br d (11.0)	4.95, dd (11.0, 1.4)	4.94, dd (10.9, 1.4)	4.95, dd (11.0, 1.0)
17	1.01, s	1.05, s	1.01, s	1.05, s
18	1.46, s	1.45, s	1.23, s	1.24, s
20	1.01, s	1.01, s	1.00, s	1.00, s
OMe		3.51, s		3.52, s

[a]NMR data (δ) were measured at 500 MHz in CD_3OD for **5**, **6**, and **8**, and at 600 MHz in CD_3OD for **7**.

correlations (Fig. 2) from H_3-20 to C-1, C-5, C-10, and an oxygenated quaternary carbon at C-9 (δ_C 78.5) indicated that C-9 was connected to C-10. HMBC cross peaks from H_2-6 to C-4, C-5, and C-10, and from H_2-7 to C-8 (δ_C 137.5), C-14 (δ_C 132.8), and C-9 suggested that C-6 was attached to C-5, and the olefinic C-8 was connected to both C-7 and C-9, establishing a cyclohexane of B ring moiety with an exocyclic olefin at C-8/C-14 fused to the A ring unit at C-5/C10. Further HMBC correlations from H_2-11 to C-8, C-9, and C-10 indicated that C-11 was connected to C-9. HMBC correlations from H_3-17 to C-12, C-13, C-14, and C-15 (δ_C 146.6) led to the connections of C-12, C-14, C-15, and C-17 to C-13, establishing the C-8/C-9 fused cyclohexene of C ring unit with a methyl and a vinyl group both attached to C-13. The relative configuration of **10** was similar as that of **7** according to NOESY correlations of H-11β (δ_H 1.71) with H_3-20 and H-15 and of H_3-18 with H-3α (δ_H 1.88), H-3β (δ_H 1.52), and H-6α (δ_H 1.92). Thus, **10** was established as 5α, 9α-dihydroxy-pimarane-8(14), 15-dien-19-oic acid and named calcarisporic acid J.

Compound **11** possessed the same molecular formula as **9**, $C_{20}H_{30}O_4$, deduced from negative HR-ESI-MS at *m/z* 333.2077 $[M–H]^-$ (Calcd. for $C_{20}H_{29}O_4$, 333.2071). The NMR spectroscopic data (Tables 1 and 4) of **11** closely resembled those of **9** except for minor differences in signals due to C-12, C-14, and C-17, suggesting that **11** was the C-13 and C-14 diastereomer of **9**. This speculation was supported by NOESY experiment. NOESY cross peaks (Fig. 3) of H-11β (δ_H 2.03) with H_3-20 and H_3-17 implied that the methyl at C-13 had a β-configuration. Correlations of H-14 (δ_H 3.22) with H_3-17 indicated that H-14 was in the β-equatorial configuration. Therefore, **11** was established as 3α,14α-dihydroxy-isopimarane-8(9), 15-dien-19-oic acid and designated as calcarisporic acid K.

Compound **12** possessed the same molecular formula of $C_{20}H_{30}O_4$ as **7**, which were determined by negative HR-ESI-MS at *m/z* 333.2084 $[M–H]^-$ (Calcd. for $C_{20}H_{29}O_4$, 333.2071). A detailed comparison of the NMR spectroscopic data (Tables 1 and 4) of **12** with those of **7** revealed that they possessed the identical planar structure, while weak differences were attributed to C-12, C-14, C-15, and C-17, suggesting that the two compounds were diastereomers. This was further verified by NOESY correlations of H-11β (δ_H 2.02) with H_3-20 and H_3-17, and of H-14 (δ_H 3.30) with H_3-17. Thus, **12** was elucidated as 5α,14α-dihydroxy-isopimarane-8(9), 15-dien-19-oic acid and designated as calcarisporic acid L.

The known compounds were identified as hawaiinolide G[14] (**13**) and 14-epi-zythiostromic acid B[16] (**14**), respectively, by comparing their NMR spectroscopic data with those reported in literatures.

It was worth mentioning that the pimarane and isopimarane type diterpenes (**5–12**) were isolated from the genus *Calcarisporium* for the first time. This discovery further supported the proposed pathway for the biosynthesis of these diterpenes (Scheme 1), where they could be synthesized from the same diterpene biosynthetic gene cluster, and the cassane and cleistanthane type diterpenoids both derived from the (*iso*) pimaranes, in which migration of either the C-13 methyl or vinyl group to C-14 led to the cassane or cleistanthane type diterpenoids[5,24,25]. Subsequently, three types of diterpenoids skeleton were heavily oxidized to form the characteristic diterpenoids above, encouraging us to search more diverse structures in this mutant strain.

Cytotoxic activities of compounds **1–14** were evaluated against two human cancer cell lines (MCF-7 and HepG-2) in the MTT assay, with taxol as a positive control (IC_{50} 5.0$\pm$0.6, 3.5$\pm$0.4 nmol/L, respectively). None of them exhibited significant activities in the concentration range of 10^{-5}–10^{-7} mol/L.

The matrix metalloproteinases (MMPs) family can degrade various protein components in the extracellular matrix and plays a key role in tumor invasion and metastasis[26,27]. Therefore, we tested the inhibitory effects of the isolated compounds on the expression of

Table 4 ^{1}H NMR spectroscopic data (δ) for compounds **9–12**[a] (δ in ppm, J in Hz).

No.	9	10	11	12
1	1.56, overlap	1.61, dd (13.6, 3.7)	1.54, overlap	1.76, overlap
	1.52, overlap	1.31, br d (13.6)		1.45, overlap
2	2.17, m	1.99, dd (13.5, 3.8)	2.19, m	1.98, overlap
	1.63, m	1.48, overlap	1.63, dd (14.4, 3.0)	1.45, overlap
3	4.00, t (2.50)	1.88, d (14.0)	4.01, br s	1.85, d (13.2)
		1.52, overlap		1.69, m
5	1.79, d (12.2)		1.79, dd (9.3, 3.9)	
6	1.90, overlap	2.54, td (13.9, 6.0)	2.02, overlap	2.45, overlap
	1.84, td (12.1, 5.3)	1.92, dd (14.7, 5.2)	1.90, overlap	1.95, overlap
7	2.34, m	2.32, tdd (13.5, 5.8, 2.2)	2.47, br d (13.5)	2.43, overlap
	1.95, dd (18.0, 4.5)	2.22, dd (15.5, 4.9)	1.86, overlap	2.08, overlap
11	2.07, m	1.71, m	2.03, overlap	2.02, overlap
	1.92, overlap	1.50, overlap	1.91, overlap	1.93, overlap
12	1.57, overlap	1.59, overlap	1.73, m	1.74, m
	1.43, m	1.49, overlap	1.36, br d (12.3)	1.38, dd (12.9, 5.0)
14	3.63, br s	5.37, br s	3.22, br s	3.30, br s
15	5.86, dd (17.7, 10.9)	5.70, dd (17.4, 10.5)	6.00, dd (18.0, 10.5)	6.01, dd (17.4, 10.4)
16	4.98, dd (17.7, 1.1)	4.96, dd (10.5, 1.7)	5.00, dd (18.0, 1.0)	5.01, dd (17.4, 1.5)
	4.94, dd (10.9, 1.1)	4.91, dd (17.4, 1.7)	4.99, dd (10.5, 1.0)	5.00, dd (10.4, 1.5)
17	0.98, s	1.03, s	0.89, s	0.92, s
18	1.27, s	1.28, s	1.28, s	1.23, s
20	0.92, s	0.95, s	0.96, s	1.06, s

[a]NMR data (δ) were measured at 500 MHz in CD_3OD for **9–12**.

MMP1 and MMP2 in human breast cancer (MCF-7) cells by Western blot assay. Due to the sample limitation, compounds **2**, **4**, **6**, and **7** were evaluated for this inhibitory activity firstly. Experimental results (Fig. 5) indicated that the four tested compounds had no significant inhibitory effects on the viability of MCF-7 cells, but the expression level of MMP1 and MMP2 could be affected obviously. Western blot showed that both **2** and **4** could reduce MMP2 expression significantly at 200 μmol/L for 24 h with significant difference from that in DMSO control group. Meanwhile, **4** could also reduce MMP1 expression significantly. This indicated that the activities of **2** and **4** may be associated with expression inhibition of MMP proteinases family, and although **2** and **4** exhibited no cytotoxicities against tested tumor cell lines, they could function in suppressing tumor invasion and metastasis and possesses potential antitumor value. Comparing the structure of **4** with that of **2**, the major difference was that a vinyl group at C-14 in **4** and a methyl group at C-14 in **2** were observed. Both **4** and **2** possessed an unsaturated unit connected to C-13. These suggested that the vinyl group attached to C-14 contributed as a functional group and the substituted group at C-14 may play an important role in the inhibitory effect on the expression level of MMP1 and MMP2.

In addition, compounds **1–14** were assessed for their anti-inflammatory inhibitory activities against the lipopolysaccharide (LPS)-induced NO production in murine microglial BV2 cells as well as their antioxidant activities against rat liver microsomal lipid peroxidation induced by Fe^{2+}-cystine *in vitro*. All compounds were inactive for anti-inflammatory and antioxidant activities at the concentrations of 10^{-5} and 10^{-4} mol/L, respectively.

3. Conclusions

Twelve new diterpenoids, calcarisporic acids A–L, including three cassanes (**1–3**), one cleistanthane (**4**), six pimaranes (**5–10**), and two isopimaranes (**11** and **12**) along with two know cleistanthanes analogues (**13** and **14**), were isolated from the mutant strain Δ*hdaA* of *Calcarisporium arbuscula*, in which an encoding histone deacetylase gene (and *hdaA*) was deleted. Compounds **5–12** are the first examples of pimarane and isopimarane type diterpenes isolated from the genus *Calcarisporium*. In addition, the inhibitory effects of four compounds (**2**, **4**, **6** and **7**) on the expression of MMP1 and MMP2 in MCF-7 cells were evaluated. Compounds **2** and **4** significantly inhibited the expression level of MMP1 and MMP2, and are promising as a potential anti-metastatic agent for the treatment of human breast cancer. Our results further present the potential of genome mining-guided discovery of bioactive natural products in fungi.

4. Experimental

4.1. General experimental procedures

Optical rotations were measured on an Autopol IV automatic polarimeter (Rudolph Research Co.). UV spectra were measured on a JASCO V650 spectrophotometer. CD spectra were measured on a JASCO J-815 spectrometer. IR spectra were recorded on a Nicolet 5700 FT-IR spectrometer using a FT-IR microscope transmission method. NMR spectra were recorded at 600 or 500 MHz for ^{1}H NMR and 150 or 125 MHz for ^{13}C NMR, respectively, on a Bruker AVIIIHD 600 (Bruker Corp., Karlsruhe, Germany) or a VNS-600 or an Inova 500 instrument (Varian Associates Inc., Palo Alto, CA, USA) in CD_3OD or DMSO-d_6 with solvent peaks used as references at 25 °C. ESI-MS and analytical HPLC were performed on a Waters ACQUITY H-Class UPLC–MS with QDA mass detector (ACQUITY UPLC® BEH, 1.7 μm, 50 mm × 2.1 mm, C18 column) using positive and negative mode electrospray ionization. HR-ESI-MS data were taken on an Agilent 6520 Accurate-Mass Q-TOF LC/MS spectrometer (Agilent Technologies, Ltd., Santa Clara, CA, USA).

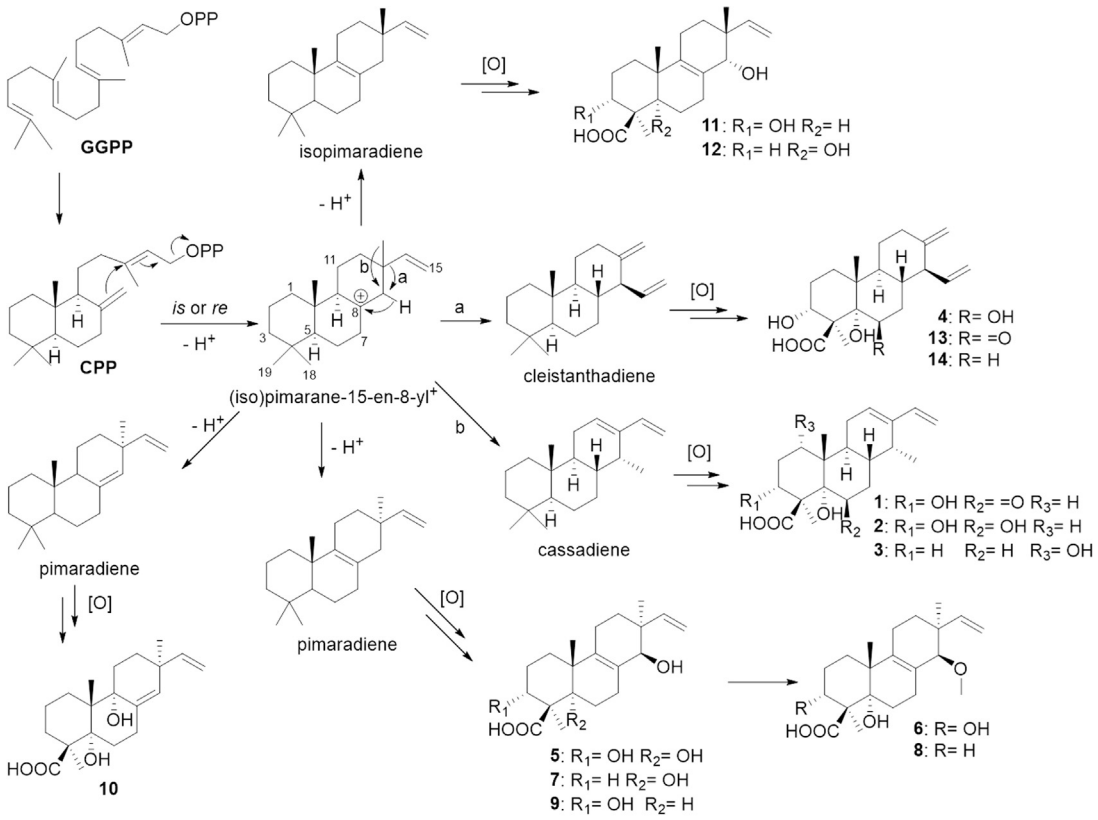

Scheme 1 Proposed biosynthetic pathways for compounds **1**–**14**.

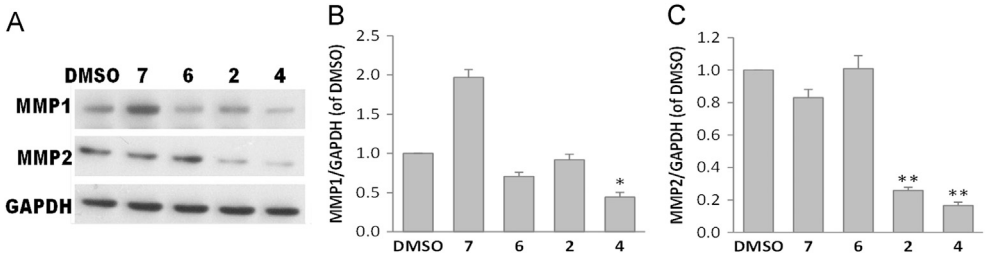

Figure 5 Effects of compounds **2**, **4**, **6**, and **7** on the expressions of MMP1 and MMP2 in MCF-7 cells. (A) Cells were treated with different test compounds at 200 μmol/L or DMSO as control for 24 h. The expressions of MMP1 and MMP2 were determined by Western blot. Representative immunoblots are shown and GAPDH is the loading control. (B) Relative expression level of MMP1 is calibrated by GAPDH. (C) Relative expression level of MMP2 is calibrated by GAPDH. Each value represents the mean ± SD of three independent experiments. $^*P<0.05$, $^{**}P<0.01$ *versus* DMSO control.

Semi-preparative HPLC was performed on a LabAlliance Series III pump equipped with a LabAlliance model 201 UV detector, using YMC-Pack ODS-A column (250 mm × 10 mm, 5μm). Column chromatography (CC) was carried out on silica gel (200–300 mesh, Qingdao Marine Chemical Inc., Qingdao, China), Sephadex LH-20 (Pharmacia Biotech AB, Uppsala, Sweden), or reversed phase C18 silica gel (50 μm, YMC, Kyoto, Japan). TLC was carried out on glass precoated silica gel GF_{254} plates (Qingdao Marine Chemical Co., Ltd., China). Spots were visualized under UV light or by spraying with 10% H_2SO_4 in 95% EtOH followed by heating.

4.2. Fungal material

Fungus *Calcarisporium arbuscula* NRRL 3705 (ATCC® 46034™) is the wild type strain. The Δ*hdaA* mutants were constructed by replacement of *hdaA* by *hph* (Hygromycin resistance gene)[5]. The mutant strains were grown on 20 L of solid PDA media (BD) divided into 200 large 150 × 15 mm^2 Petri dishes at room temperature for 40 days.

4.3. Extraction and isolation

The fermented material was extracted repeatedly with EtOAc (3 × 5.0 L), and the organic solvent was evaporated to dryness under vacuum to afford the crude extract (14.2 g), which was partitioned between MeOH and hexane. The MeOH fraction (13.5 g) was evaporated to dryness under vacuum, and separated by reversed phase C18 silica gel vacuum liquid chromatography with a gradient of MeOH (20%–100%) in H_2O to give eleven fractions (F1–F11).

Fractions F3–F5 were combined (4.1 g) and subjected to reversed phase C18 silica gel vacuum liquid chromatography with a gradient of MeOH (5–80%) in H_2O to afford twenty fractions (F3-1–F3-20). Fraction F3-15 (307 mg) was separated by reverse-phase HPLC (YMC-ODS-A, 5 μm, 250 mm × 20 mm), eluted by 42% MeCN–H_2O (*v/v*, 0.02% formic acid) at a flow rate of 5.0 mL/min detected at 210 nm, to give six fractions (F3-15-1–F3-15-6). Fraction F3-15-2 (30.2 mg) was further purified by reverse-phase HPLC, eluted by 72% MeOH–H_2O (*v/v*, 0.01% trifluoroacetic acid) at a flow rate of 2.0 mL/min detected at 210 nm, to yield **5** (16.1 mg, t_R = 22 min). Fraction F3-15-3 (18.2 mg) was further purified by reverse-phase HPLC, eluted by 75% MeOH –H_2O (*v/v*, 0.01% trifluoroacetic acid) at a flow rate of 2.0 mL/min detected at 210 nm, to yield **11** (1.9 mg, t_R = 14 min) and **9** (8.9 mg, t_R = 19 min). Fraction F3-18 (472 mg) was subjected to CC over Sephadex LH-20 eluted by MeOH to afford nine fractions (F3-18-1–F3-18-9). Fraction F3-18-5 (90 mg) was purified by reverse-phase HPLC, eluted by 63% MeCN–H_2O (*v/v*, 0.02% formic acid) at a flow rate of 2.0 mL/min detected at 210 nm, to yield **7** (21.8 mg, t_R = 17 min), **6** (12.6 mg, t_R = 19 min), **8** (8.3 mg, t_R = 34 min), and **13** (2.3 mg, t_R = 42 min). Fraction F3-18-7 (65 mg) was purified by reverse-phase HPLC, eluted by 57% MeCN–H_2O (*v/v*, 0.02% formic acid) at a flow rate of 2.0 mL/min detected at 210 nm, to yield **1** (1.5 mg, t_R = 36 min).

Fraction F6 (1.6 g) was subjected to CC over Sephadex LH-20 eluted by MeOH to afford seven fractions (F6-1–F6-7). Fraction F6-6 (1.1 g) was recrystallized with MeOH to give a white solid, which was further purified by reverse-phase HPLC, eluted by 50% MeCN –H_2O (*v/v*, 0.01% trifluoroacetic acid) at a flow rate of 2.0 mL/min detected at 210 nm, to give **4** (49.8 mg, t_R = 34 min). Fraction F6-7 (88 mg) was purified by reverse-phase HPLC, eluted by 50% MeCN –H_2O (*v/v*, 0.01% trifluoroacetic acid) at a flow rate of 2.0 mL/min detected at 210 nm, to give **2** (13.7 mg, t_R = 32 min) and subfraction F6-73 (13.4 mg), which was further purified by reverse-phase HPLC, eluted by 80% MeOH–H_2O (*v/v*, 0.01% trifluoroacetic acid) at a flow rate of 2.0 mL/min detected at 210 nm, to give **3** (3.8 mg, t_R = 29 min).

Fraction F8 (1.1 g) was further purified by reverse-phase HPLC (YMC-ODS-A, 5 μm, 250 × 20 mm), eluted by 47% MeCN–H_2O (*v/v*, 0.02% formic acid) at a flow rate of 5.0 mL/min detected at 210 nm, to give six fractions (F8-1–F8-6). Fraction F8-4 (7.0 mg) was purified by reverse-phase HPLC, eluted by 47% MeCN–H_2O (*v/v*, 0.02% formic acid) at a flow rate of 2.0 mL/min detected at 210 nm, to give **10** (3.6 mg, t_R = 53 min). Fraction F8-5 (270 mg) was further purified by Sephadex LH-20 eluted by MeOH to give **14** (8.0 mg). Fraction F8-6 (89 mg) was further purified by reverse-phase HPLC, eluted by 50% MeCN–H_2O (*v/v*, 0.02% formic acid) at a flow rate of 2.0 mL/min detected at 210 nm, to give **12** (5.2 mg, t_R = 24 min).

4.3.1. *Calcarisporic acid A (**1**)*

Colorless amorphous solid; $[\alpha]_D^{20}$ +30.0 (*c* 0.10, MeOH); UV (MeOH) λ_{max} (logε) 229 (4.68) nm; CD (*c* 1.4 × 10^{-3} mol/L, MeOH) λ_{max} ($\Delta\varepsilon$) 240 (−0.29), 288 (+0.13), 320 (−0.12) nm; IR ν_{max} 3490, 3086, 2930, 1809, 1724, 1649, 1603, 1457, 1391, 1223, 1099, 994, 897, 852, 760 cm^{-1}; ^1H NMR (CD_3OD, 500 MHz) data see Table 2, ^{13}C NMR (CD_3OD, 125 MHz) data see Table 1; ESI-MS *m/z* 347 $[M–H]^-$; HR-ESI-MS: *m/z* 347.1864 $[M–H]^-$ (Calcd. for $C_{20}H_{27}O_5$, 347.1864).

4.3.2. *Calcarisporic acid B (**2**)*

Colorless granules (MeOH); $[\alpha]_D^{20}$ +51.7 (*c* 0.19, MeOH); UV (MeOH) λ_{max} (logε) 231 (4.96) nm; IR ν_{max} 3307, 3198, 2938, 2612, 1694, 1652, 1602, 1516, 1468, 1436, 1276, 1081, 1004, 955, 893, 769, 732, 592 cm^{-1}; ^1H NMR (DMSO-d_6, 600 MHz) data see Table 2, ^{13}C NMR (DMSO-d_6, 150 MHz) data see Table 1; ESI-MS *m/z* 349 $[M–H]^-$; HR-ESI-MS: *m/z* 349.2030 $[M–H]^-$ (Calcd. for $C_{20}H_{29}O_5$, 349.2020).

4.3.3. *Calcarisporic acid C (**3**)*

Colorless amorphous solid; $[\alpha]_D^{20}$ +83.3 (*c* 0.19, MeOH); UV (MeOH) λ_{max} (logε) 231 (4.81) nm; IR ν_{max} 3309, 3183, 2974, 2930, 1688, 1652, 1606, 1462, 1271, 1117, 962, 949, 929, 893, 798, 711, 647, 535 cm^{-1}; ^1H NMR (DMSO-d_6, 600 MHz) data see Table 2, ^{13}C NMR (DMSO-d_6, 150 MHz) data see Table 1; ESI-MS *m/z* 333 $[M–H]^-$; HR-ESI-MS: *m/z* 333.2083 $[M–H]^-$ (Calcd. for $C_{20}H_{29}O_4$, 333.2071).

4.3.4. *Calcarisporic acid D (**4**)*

Colorless needles (MeOH); $[\alpha]_D^{20}$ +10.2 (*c* 0.17, MeOH); UV (MeOH) λ_{max} (logε) 204 (4.50) nm; IR ν_{max} 3456, 3367, 3073, 2965, 2320, 1694, 1645, 1509, 1465, 1421, 1297, 1166, 1003, 965, 918, 771, 725, 608, 568 cm^{-1}; ^1H NMR (DMSO-d_6, 600 MHz) data see Table 2, ^{13}C NMR (DMSO-d_6, 150 MHz) data see Table 1; ESI-MS *m/z* 349 $[M–H]^-$; HR-ESI-MS: *m/z* 349.2031 $[M–H]^-$ (Calcd. for $C_{20}H_{29}O_5$, 349.2020).

4.3.5. *Calcarisporic acid E (**5**)*

Colorless amorphous solid; $[\alpha]_D^{20}$ −12.0 (*c* 0.20, MeOH); UV (MeOH) λ_{max} (logε) 206 (4.37) nm; IR ν_{max} 3339, 3080, 2935, 1701, 1638, 1460, 1380, 1267, 1009, 948, 912, 855, 706, 672 cm^{-1}; ^1H NMR (CD_3OD, 500 MHz) data see Table 3, ^{13}C NMR (CD_3OD, 150 MHz) data see Table 1; ESI-MS *m/z* 349 $[M–H]^-$; HR-ESI-MS: *m/z* 349.2036 $[M–H]^-$ (Calcd. for $C_{20}H_{29}O_5$, 349.2020).

4.3.6. *Calcarisporic acid F (**6**)*

Colorless amorphous solid; $[\alpha]_D^{20}$ −21.0 (*c* 0.13, MeOH); UV (MeOH) λ_{max} (logε) 204 (4.58) nm; IR ν_{max} 3495, 3274, 3079, 2934, 1701, 1635, 1461, 1383, 1238, 1089, 1005, 939, 907, 864, 690, 665 cm^{-1}; ^1H NMR (CD_3OD, 500 MHz) data see Table 3, ^{13}C NMR (CD_3OD, 125 MHz) data see Table 1; ESI-MS *m/z* 363 $[M–H]^-$; HR-ESI-MS: *m/z* 363.2182 $[M–H]^-$ (Calcd. for $C_{21}H_{31}O_5$, 363.2177).

4.3.7. *Calcarisporic acid G (**7**)*

Colorless needles (MeOH); $[\alpha]_D^{20}$ +16.0 (*c* 0.20, MeOH); UV (MeOH) λ_{max} (logε) 204 (4.47) nm; IR ν_{max} 3544, 3353, 2934, 1686, 1621, 1467, 1433, 1377, 1280, 1255, 1065, 941, 914, 800, 675 cm^{-1}; ^1H NMR (CD_3OD, 600 MHz) data see Table 3, ^{13}C NMR (CD_3OD, 150 MHz) data see Table 1; ESI-MS *m/z* 333 $[M–H]^-$; HR-ESI-MS: *m/z* 333.2077 $[M–H]^-$ (Calcd. for $C_{20}H_{29}O_4$, 333.2071).

4.3.8. *Calcarisporic acid H (**8**)*

Colorless amorphous solid; $[\alpha]_D^{20}$ +12.0 (*c* 0.15, MeOH); UV (MeOH) λ_{max} (logε) 205 (4.51) nm; IR ν_{max} 3570, 3147, 2937, 1724, 1638, 1606, 1458, 1383, 1274, 1200, 1073, 973, 937, 854, 796, 675 cm^{-1}; ^1H NMR (CD_3OD, 500 MHz) data see Table 3, ^{13}C NMR (CD_3OD, 125 MHz) data see Table 1; ESI-MS *m/z* 347 $[M–H]^-$; HR-ESI-MS: *m/z* 347.2239 $[M–H]^-$ (Calcd. for $C_{21}H_{31}O_4$, 347.2228).

4.3.9. *Calcarisporic acid I (**9**)*

Colorless amorphous solid; $[\alpha]_D^{20}$ +56.9 (*c* 0.19, MeOH); UV (MeOH) λ_{max} (logε) 206 (4.50) nm; IR ν_{max} 3427, 3082, 2933, 1694, 1456, 1379, 1250, 1197, 1046, 966, 915, 858, 698 cm^{-1}; ^1H NMR (CD_3OD, 500 MHz) data see Table 4, ^{13}C NMR (CD_3OD, 125 MHz) data see Table 1; ESI-MS *m/z* 333 $[M–H]^-$; HR-ESI-MS: *m/z* 333.2077 $[M–H]^-$ (Calcd. for $C_{20}H_{29}O_4$, 333.2071).

4.3.10. *Calcarisporic acid J (**10**)*

Colorless amorphous solid; $[\alpha]_D^{20}$ +103.9 (*c* 0.22, MeOH); UV (MeOH) λ_{max} (logε) 205 (4.41) nm; IR ν_{max} 3382, 2950, 2875, 1700, 1637, 1553, 1453, 1377, 1254, 1143, 1090, 999, 917, 882, 802, 656 cm^{-1}; ^1H NMR (CD_3OD, 500 MHz) data see Table 4, ^{13}C NMR (CD_3OD, 125 MHz) data see Table 1; ESI-MS *m/z* 333 $[M–H]^-$; HR-ESI-MS: *m/z* 333.2069 $[M–H]^-$ (Calcd. for $C_{20}H_{29}O_4$, 333.2071).

4.3.11. *Calcarisporic acid K (**11**)*

Colorless amorphous solid; $[\alpha]_D^{20}$ +85.9 (*c* 0.16, MeOH); UV (MeOH) λ_{max} (logε) 204 (4.52) nm; IR ν_{max} 3430, 3082, 2928, 2871, 1693, 1455, 1413, 1378, 1357, 1199, 1146, 1005, 980, 913, 802, 698, 621 cm^{-1}; ^1H NMR (CD_3OD, 500 MHz) data see Table 4, ^{13}C NMR (CD_3OD, 125 MHz) data see Table 1; ESI-MS *m/z* 333 $[M–H]^-$; HR-ESI-MS: *m/z* 333.2077 $[M–H]^-$ (Calcd. for $C_{20}H_{29}O_4$, 333.2071).

4.3.12. *Calcarisporic acid L (**12**)*

Colorless amorphous solid; $[\alpha]_D^{20}$ +126.9 (*c* 0.12, MeOH); UV (MeOH) λ_{max} (logε) 204 (4.59) nm; IR ν_{max} 3498, 2930, 2865, 1707, 1639, 1458, 1391, 1308, 1278, 1002, 981, 917, 798, 685 cm^{-1}; ^1H NMR (CD_3OD, 500 MHz) data see Table 4, ^{13}C NMR (CD_3OD, 125 MHz) data see Table 1; ESI-MS *m/z* 333 $[M–H]^-$; HR-ESI-MS: *m/z* 333.2084 $[M–H]^-$ (Calcd. for $C_{20}H_{29}O_4$, 333.2071).

4.4. *Cytotoxicity assay*

Compounds **1**–**14** were tested for cytotoxic activities against MCF-7 (human breast cancer) and HepG-2 (human liver cancer) cell lines by the MTT method, as described in the literature[28].

4.5. *Inhibitory effects on the expression of MMP1 and MMP2 in MCF-7 cells*

Compounds **2**, **4**, **6**, and **7** were tested for the inhibitory effects on the expression of MMP1 and MMP2 in human breast carcinoma cell line MCF-7 by Western blot. MCF-7 cells was purchased from Cell Bank of Shanghai Institute of Biochemistry and Cell Biology, Chinese Academy of Science, and was cultured in DMEM medium (Gibco, Invitrogen Corporation) supplemented with 10% heat-inactivated fetal bovine serum (FBS), 100 U/mL benzyl penicillin G, and 100 mg/L streptomycin under a humidified atmosphere of 5% CO_2 at 37 °C for 24 h. MCF-7 cells were treated with different test compounds at 200 μmol/L or DMSO as control for 24 h. Then, cells were collected and lysed. The lysates were clarified by 12,000 × *g* centrifugation at 4 °C for 30 min. Total proteins were quantified with a microplate spectrophotometer using the bicinchoninic acid assay (BCA assay). Then equal amount of proteins were separated by SDS-polyacrylamide gel (SDS-PAGE) and transferred onto PVDF membranes (Millipore, Bedford, MA, USA). The blots were incubated with primary antibodies overnight at 4 °C, followed by second antibodies at the room temperature for 0.5 h. Immunoreactive protein bands were detected by the ECL detection system (Amersham Bioscience, Piscataway, NJ, USA).

4.6. *Anti-inflammatory activity assay*

Compounds **1**–**14** were assessed for their anti-inflammatory inhibitory activities against the lipopolysaccharide (LPS) induced NO production in murine microglial BV2 cell line using the Griess method, as described in the literature[29]. Curcumin was used as the positive control (inhibitory rate 66.0 ± 2.5% at 10^{-5} mol/L).

4.7. *Antioxidant assay*

Compounds **1**–**14** were assessed for their antioxidant activities against rat liver microsomal lipid peroxidation induced by Fe^{2+}–cystine *in vitro*, as described in the literature[30]. Curcumin was used as the positive control (inhibitory rate 95.0 ± 3.5% at 10^{-4} mol/L).

Acknowledgments

This work was supported financially by National Natural Science Foundation of China (Nos. 21502233 and 81522043), CAMS Initiative for Innovative Medicine (CAMS-I2M-1-010), the PUMC Youth Fund (33320140175), and the State Key Laboratory Fund for Excellent Young Scientists to Youcai Hu (GTZB201401). We are grateful to the Department of Instrumental Analysis, Institute of Materia Medica, Chinese Academy of Medical Sciences & Peking Union Medical College for the spectroscopic measurements and Prof. Xiaoguang Chen and Prof. Dan Zhang for the cytotoxicity, anti-inflammatory, and antioxidant assays.

Appendix A. Supplementary material

Supplementary data associated with this article can be found in the online version at https://doi.org/10.1016/j.apsb.2017.12.012.

References

1. Watson P. Calcarisporium arbuscula living as an endophyte in apparently healthy sporophores of Russula and Lactarius. *Trans Br Mycol Soc* 1955;**38**:409–14.
2. Osselton MD, Baum H, Beechey RB. Isolation, purification and characterization of aurovertin B. *Biochem Soc Trans* 1974;**2**:200–2.
3. van Raaij MJ, Abrahams JP, Leslie AG, Walker JE. The structure of bovine F1-ATPase complexed with the antibiotic inhibitor aurovertin B. *Proc Natl Acad Sci U S A* 1996;**93**:6913–7.
4. Mulheirn LJ, Beechey RB, Leworthy DP, Osselton MD. Aurovertin B, a metabolite of *Calcarisporium arbuscula*. *J Chem Soc Chem Commun* 1974;**21**:874–6.
5. Mao XM, Xu W, Li D, Yin WB, Chooi YH, Li YQ, et al. Epigenetic genome mining of an endophytic fungus leads to the pleiotropic biosynthesis of natural products. *Angew Chem Int Ed* 2015;**54**:7592–6.
6. Cichewicz RH. Epigenome manipulation as a pathway to new natural product scaffolds and their congeners. *Nat Prod Rep* 2010;**27**:11–22.
7. Albright JC, Henke MT, Soukup AA, McClure RA, Thomson RJ, Keller NP, et al. Large-scale metabolomics reveals a complex response of *Aspergillus nidulans* to epigenetic perturbation. *ACS Chem Biol* 2015;**10**:1535–41.

8. Wu G, Zhou H, Zhang P, Wang X, Li W, Zhang W, et al. Polyketide production of pestaloficiols and macrodiolide ficiolides revealed by manipulations of epigenetic regulators in an endophytic fungus. *Org Lett* 2016;**18**:1832–5.
9. Fan A, Mi W, Liu Z, Zeng G, Zhang P, Hu Y, et al. Deletion of a histone acetyltransferase leads to the pleiotropic activation of natural products in *Metarhizium robertsii*. *Org Lett* 2017;**19**:1686–9.
10. Zheng Y, Ma K, Lyu H, Huang Y, Liu H, Liu L, et al. Genetic manipulation of the COP9 signalosome subunit PfCsnE leads to the discovery of pestaloficins in *Pestalotiopsis fici*. *Org Lett* 2017;**19**:4700–3.
11. Li MH, Li QQ, Zhang CH, Zhang N, Cui ZH, Huang LQ, et al. An ethnopharmacological investigation of medicinal *Salvia* plants (Lamiaceae) in China. *Acta Pharm Sin B* 2013;**4**:273–80.
12. Liu N, Wang S, Lou HX. A new pimarane-type diterpenoid from moss *Pseudoleskeella papillosa* (Lindb.) Kindb. *Acta Pharm Sin B* 2012;**3**:256–9.
13. Chen S, Zhang Y, Niu S, Liu X, Che Y. Cytotoxic cleistanthane and cassane diterpenoids from the entomogenous fungus *Paraconiothyrium hawaiiense*. *J Nat Prod* 2014;**77**:1513–8.
14. Chen S, Zhang Y, Zhao C, Ren F, Liu X, Che Y. Hawaiinolides E–G, cytotoxic cassane and cleistanthane diterpenoids from the entomogenous fungus *Paraconiothyrium hawaiiense*. *Fitoterapia* 2014;**99**:236–42.
15. Morris SA, Curotto JE, Zink DL, Dreikorn S, Jenkins R, bills GF, et al. Sonomolides A and B, new broad spectrum antifungal agents isolated from a coprophilous fungus. *Tetrahedron Lett* 1995;**36**:9101–4.
16. Shiono Yoshihito, Ogata Kota, Koseki Takuya, Murayama Tetsuya, Funakoshi T. A cleistanthane diterpene from a marine-derived *Fusarium* species under submerged fermentation. *Z Naturforsch* 2010;**65b**:753–6.
17. Li F, Ma J, Li CJ, Yang JZ, Zhang D, Chen XG, et al. Bioactive isopimarane diterpenoids from the stems of *Euonymus oblongifolius*. *Phytochemistry* 2017;**135**:144–50.
18. Allard PM, Martin MT, Dau ME, Leyssen P, Gueritte F, Litaudon M. Trigocherrin A, the first natural chlorinated daphnane diterpene orthoester from *Trigonostemon cherrieri*. *Org Lett* 2012;**14**:342–5.
19. Zhang L, Luo RH, Wang F, Jiang MY, Dong ZJ, Yang LM, et al. Highly functionalized daphnane diterpenoids from *Trigonostemon thyrsoideum*. *Org Lett* 2010;**12**:152–5.
20. Zhang L, Luo RH, Wang F, Dong ZJ, Yang LM, Zheng YT, et al. Daphnane diterpenoids isolated from *Trigonostemon thyrsoideum* as HIV-1 antivirals. *Phytochemistry* 2010;**71**:1879–83.
21. Kirk DN. The chiroptical properties of carbonyl compounds. *Tetrahedron* 1986;**42**:777–818.
22. Bai J, Chen H, Fang ZF, Yu SS, Wang WJ, Liu Y, et al. Sesquiterpenes from the roots of *Illicium dunnianum*. *Phytochemistry* 2012;**80**:137–47.
23. Ayer WA, Khan AQ. Zythiostromic acids, diterpenoids from an antifungal *Zythiostroma* species associated with aspen. *Phytochemistry* 1996;**42**:1647–52.
24. Peters RJ. Two rings in them all: the labdane-related diterpenoids. *Nat Prod Rep* 2010;**27**:1521–30.
25. Gao Y, Honzatko RB, Peters RJ. Terpenoid synthase structures: a so far incomplete view of complex catalysis. *Nat Prod Rep* 2012;**29**:1153–75.
26. Khasigov PZ, Podobed OV, Gracheva TS, Salbiev KD, Grachev SV, Berezov TT. Role of matrix metalloproteinases and their inhibitors in tumor invasion and metastasis. *Biochemistry* 2003;**68**:711–7.
27. Park M, Han J, Lee CS, Soo BH, Lim KM, Ha H. Carnosic acid, a phenolic diterpene from rosemary, prevents UV-induced expression of matrix metalloproteinases in human skin fibroblasts and keratinocytes. *Exp Dermatol* 2013;**22**:336–41.
28. Ma S-G, Tang W-Z, Liu Y-X, Hu Y-C, Yu S-S, Zhang Y, et al. Prenylated C6–C3 compounds with molecular diversity from the roots of *Illicium oligandrum*. *Phytochemistry* 2011;**72**:115–25.
29. Qu J, Fang L, Ren X-D, Liu Y, Yu S-S, Li L, et al. Bisindole alkaloids with neural anti-inflammatory activity from *Gelsemium elegans*. *J Nat Prod* 2013;**76**:2203–9.
30. Hu Y, Ma S, Li J, Yu S, Qu J, Liu J, et al. Targeted isolation and structure elucidation of stilbene glycosides from the bark of *Lysidice brevicalyx* Wei guided by biological and chemical screening. *J Nat Prod* 2008;**71**:1800–5.